

Flexible 3D pharmacophores as descriptors of dynamic biological space

James H. Nettles^{a,*}, Jeremy L. Jenkins^a, Chris Williams^b, Alex M. Clark^b,
Andreas Bender^a, Zhan Deng^a, John W. Davies^a, Meir Glick^a

^a Lead Discovery Informatics, Lead Discovery Center, Novartis Institutes for BioMedical Research Inc.,
250 Massachusetts Ave., Cambridge, MA 02139, United States

^b Chemical Computing Group Inc., 1010 Sherbrooke Street West, Suite 910 Montreal, Quebec H3A 2R7, Canada

Accepted 26 February 2007

Available online 1 March 2007

Abstract

Development of a pharmacophore hypothesis related to small-molecule activity is pivotal to chemical optimization of a series, since it defines features beneficial or detrimental to activity. Although crystal structures may provide detailed 3D interaction information for one molecule with its receptor, docking a different ligand to that model often leads to unreliable results due to protein flexibility. Graham Richards' lab was one of the first groups to utilize “fuzzy” pattern recognition algorithms taken from the field of image processing to solve problems in protein modeling. Thus, descriptor “fuzziness” was partly able to emulate conformational flexibility of the target while simultaneously enhancing the speed of the search. In this work, we extend these developments to a ligand-based method for describing and aligning molecules in flexible chemical space termed FEature POint PharmacophoreS (FEPOPS), which allows exploration of dynamic biological space. We develop a novel, combinatorial algorithm for molecular comparisons and evaluate it using the WOMBAT dataset. The new approach shows superior retrospective virtual screening performance than earlier shape-based or charge-based algorithms. Additionally, we use target prediction to evaluate how FEPOPS alignments match the molecules biological activity by identifying the atoms and features that make the key contributions to overall chemical similarity. Overall, we find that FEPOPS are sufficiently fuzzy and flexible to find not only new ligand scaffolds, but also challenging molecules that occupy different conformational states of dynamic biological space as from induced fits.

© 2007 Elsevier Inc. All rights reserved.

Keywords: Pharmacophore; FEPOPS; Virtual screening; 3D descriptors; Chemical space; Biological space

1. Introduction

Scientific information has dramatically expanded during the past decade. Researchers have sequenced the human genome [1] accessed expression information on a chip [2] and garnered structural insight from complex biomolecular machines like G-protein coupled receptors [3] and structural proteins [4,5].

Advances in robotics, computational hardware and software allow production of staggering numbers of complex new chemical entities and biological readouts of their effects. For drug discovery, these are steps in the right direction, but effectively utilizing this glut of information still has not reached its potential [6]. Thinking of connecting complex signaling and metabolic networks, predicting three-dimensional structures of

receptors or addressing conformational flexibility of biological macromolecules in the presence of different ligands may suffice to illustrate challenges still ahead. The development of enhanced tools, which allow researchers to effectively analyze trends in this multifarious environment, has necessarily become its own important arena for study.

A novel feature of Graham Richards' research was the utilization of algorithms from the field of signal and image processing to enhance *in silico* drug discovery. He explored these methods' ability to scale back non-essential information and reveal the underlying patterns in complex molecular data sets as they do for other physical phenomenon. In 2002, a multi-scale approach was first successfully implemented to identify binding sites on the surface of proteins [7] and to dock flexible molecules [8]. In the multi-scale approach used, a hierarchy of models was generated using a *k*-means clustering algorithm for the potential ligand, which was represented by a growing number of feature points. These works demonstrated that

* Corresponding author. Tel.: +1 617 871 3904.

E-mail address: James.nettles@novartis.com (J.H. Nettles).

docking flexible molecules using a four-point representation was sufficient enough to closely reproduce the binding mode of the ligands tested. These encouraging results are weighted against the observations that many docking algorithms perform well for some systems while very poorly for others [9]. The performance of standard docking may be increased through statistical training using multiple receptor complexes, however, these methods are limited to cases with appropriate structural data [10]. From another perspective, chemical similarity has been shown to strongly correlate with biological function. However, 2D descriptors are inherently limited to a chemical space close to the reference molecule [11,12]. We became interested in exploring 3D ligand-based methods as an adjunct to both 2D and receptor based methods. The underlying idea is that specific parts of a small molecule's flexible chemical space inherently complement aspects of the receptor's biological space they affect. It follows that those elements which correlate in chemical activity space likely result from receptor specific features. Those correlating features may be extracted as descriptors of biology that may be used with or without explicit structural constraints.

A ligand-based reincarnation of the multi-scale approach was developed at Novartis as the FEature POint PharmacophoreS (FEPOPS) algorithm [13]. FEPOPS derives a “fuzzy” molecular representation for a compound and encodes pharmacophoric properties on the feature points. This information is used for 3D similarity searching to identify novel scaffold classes (“scaffold hops”) where the similarity between query molecule and each database compound is calculated using Pearson's correlation between the feature descriptors [14]. FEPOPS was also recently employed for target identification [15] and is now used routinely for virtual screening in project work. This paper communicates recent modifications to the FEPOPS algorithm that produce improvements over the original version and allow for a more detailed analysis of individual feature contribution toward enhancing or limiting similarity.

Encoding a molecular structure for 3D similarity calculations is a non-trivial problem [11] which is, at the same time, quite subjective—what properties of the molecule should be the features of focus? Following the choice of descriptors for the molecular properties is the question of how to “align” two or more different molecules for comparison. This becomes increasingly challenging as structural similarities between the molecular pairs decreases. In the cases presented here only two “extreme” possibilities shall be discussed: aligning molecules by the *shape(s)* that can be attained, and aligning molecules by the *charges* presented to the environment.

Intuitively, shape is a very logical descriptor to relate a ligand to its binding site. Early suggestions from the Richards' lab regarding shape as a descriptor [16], found functional expressions in new algorithms, such as Rapid Overlay of Chemical Structures (ROCS), that efficiently perform shape alignment of molecules by employing Gaussian functions which enable analytical calculation of gradients. ROCS shapes provide excellent alignments in many situations and have been effectively used for virtual screening [17]. While additional

information about interaction types such as charge can be included, problems like matching of sub-shapes or aligning non-shape-based features (polar/non-polar, H-bond donor/acceptor, etc...) represent challenges for whole-shape matching algorithms such as this one.

A contrasting procedure of charge-based alignment of molecular features was chosen for the original FEPOPS method [13]. FEPOPS does not generate an explicit shape descriptor. Instead, the distances between the four or more feature points of a given molecule can provide a pseudo shape. To simplify processing, the original algorithm used relative electrostatics to determine the order of feature points and pair-wise Pearson correlations between those features to compute similarity. The features were first enumerated for the most negative charge (feature point 1), followed by the next most negative charge (feature point 2), with increasing numbers representing more electropositive centers. This algorithm has worked remarkably well in both retrospective enrichment studies and prospective drug discovery for finding actives in new regions of chemical space. However, biases were observed in cases where substitution of strongly charged groups (that were not part of the pharmacophore) caused the numbering of the feature points to be swapped on otherwise similar molecules. In those cases, it would be advantageous to have an alternative way to automatically align and match feature points.

Following the observations above, we hypothesised that both shape as well as atomic (or feature point) properties should be included in the alignment “objective function”. Using the existing feature point distances of the four-point irregular tetrahedron allowed us to capture the overall shape of most molecules to a satisfying degree, while alleviating the computational expense of computing an explicit shape descriptor. To eliminate our reliance on a single descriptor, as in the earlier version, we can now employ all seven FEPOPS descriptors for comparing molecules. Included are the distances in space between feature centroids, the atomic log *P*, hydrogen bond donor and hydrogen bond acceptor properties, atom electronegativity as well as formal negative and positive charges of the atoms (where hydrogen bond donor and acceptor properties as well as formal charges are integer properties, while the rest are represented as real values). To optimize the similarity calculation of structures, while at the same time producing a sensible alignment of molecules, we now perform combinatorial evaluation of the feature space representations of molecules. To further the interpretation of the algorithm results, we now provide output of the 3D coordinates of the FEPOPS conformers for visualization and color coded 2D schemes of the chemical structures. By understanding the mechanism involved in a scaffold hop we can glean information about the biological environment. Further details of the methods and results are presented in the following sections.

Overall, we show that using multiple descriptors and combinatorial alignment improves active recall. We are also able to use the FEPOPS color coding to identify bioisosteres or functionally equivalent groups between compounds. These can guide further compound optimization and provide clues as to what the binding mode of small molecules will be. By mapping

the pharmacophoric features to atomic cluster centroids rather than explicit atoms, and by including tautomeric/conformational flexibility for each molecule the resultant alignments accurately highlight similarity between structures that would not be found with 2D methods. Likewise, use of this tool may assist elucidation of underlying dynamic properties of flexible binding sites that are not obvious from static structural models. Given the importance of probing biological functions with small molecules, we are confident that the development of this work can guide our future understanding of interactions between chemical and biological worlds.

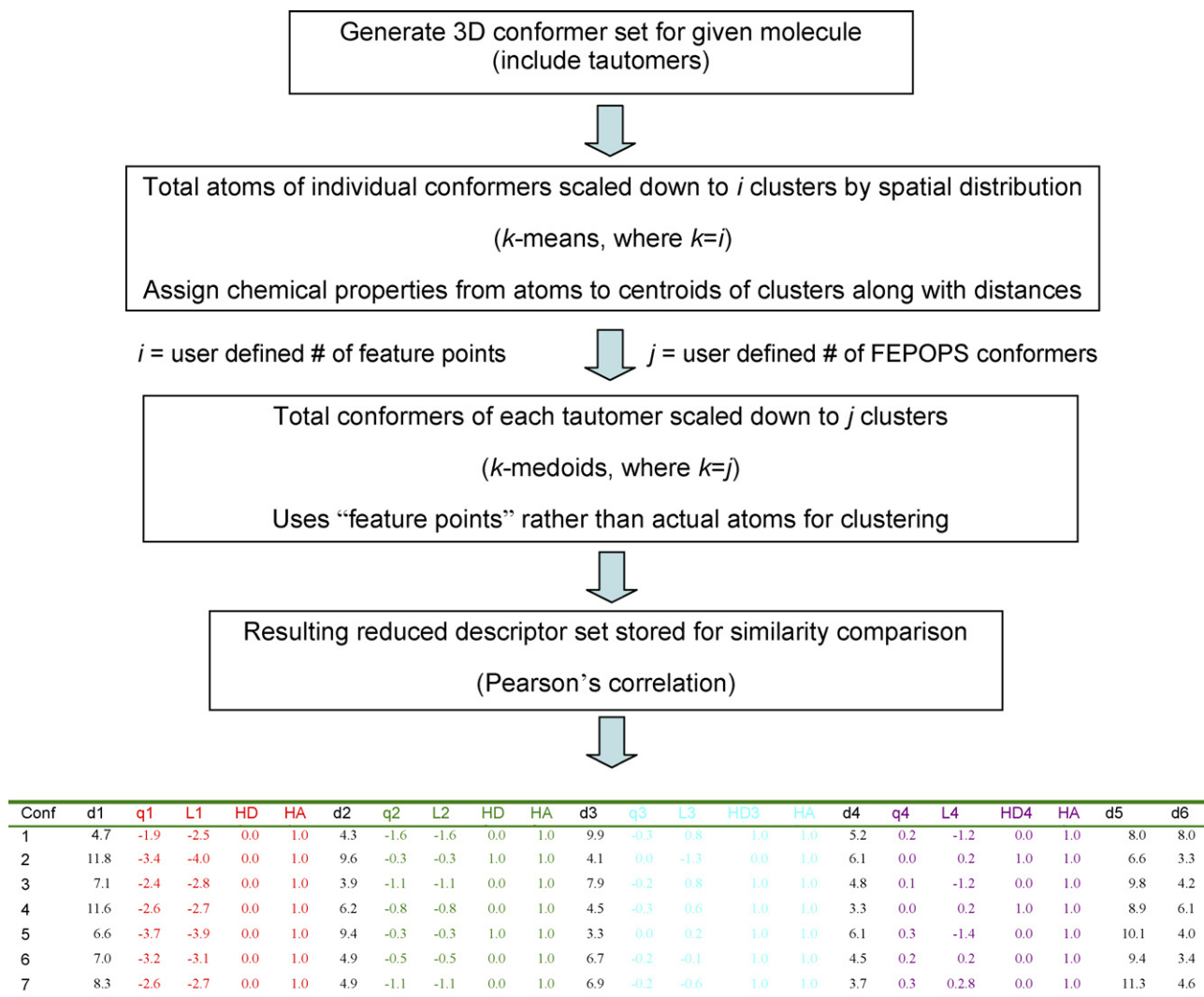
2. Methods

These methods describe two variations of the FEPOPS algorithm used to generate 3D descriptors of small molecules and one new algorithm for alignment and comparison of those descriptors. The new version of FEPOPS code (FEPOPS-II), still under development, is a JAVA application integrating conformation generation, clustering, and descriptor assignment, into a single, portable executable. FEPOPS-II has an

additional feature for accepting pools of conformers from external applications as inputs for clustering. This allows the user to choose a favorite external conformation generation method, yet use FEPOPS to scale down the flexible chemical space. Additionally, a new algorithm for combinatorial alignment (CombiAlign) is presented that can be used as a post-processor with output from either of the FEPOPS programs.

2.1. FEPOPS-I

FEPOPS descriptors were calculated using the method previously described by Jenkins et al. [13]. The core application was written in C and linking between external modules was scripted through the Pipeline Pilot interface environment [18]. The workflow of the algorithm is illustrated in Scheme 1. Molecules were first preprocessed by: (a) enumerating tautomers and generating their 3D conformations, followed by limited minimization with the Clean forcefield in Pipeline Pilot, (b) assigning protonation states at pH 7.4, (c) calculating Gasteiger–Marsili partial charges [19] and atomic log *P* values



Scheme 1. The generation of FEPOPS descriptors.

using $X \log P$ [20]. An ensemble of multiple conformers for each molecule was generated by systematic variation of rotatable bonds at a fixed angle increment as described previously. Ligand atoms were then grouped into four k -means clusters [21] based on their spatial coordinates, and a geometric centroid was defined for each cluster. Each centroid was transformed to a “feature point” through association with five different types of pharmacophoric features: the sum of partial charges within this cluster, sum of atomic $\log P$ values, presence of hydrogen bond donors and acceptors, and distances to other centroids. In order to make the computation amenable to large databases, we used k -medoids clustering to further group and select a small number (typically $k = 7$) of explicit and diverse FEPOPS conformers. The programs Partitioning Around Medoids (PAM) and Clustering of *LA*rg*E* Application (CLARA) in the R package were used to perform the k -medoids clustering calculation [22]. The selected medoid FEPOPS features were stored in a lookup table. The FEPOPS similarity between two molecules is defined as the best Pearson’s correlation coefficient between their aligned FEPOPS conformers [14].

2.2. FEPOPS-II

To more efficiently test some of the variables used by the FEPOPS-I program, new code has been produced to increase flexibility and portability. Using the same references as FEPOPS-I, computations of charge, $\log P$, handling of internal or externally generated conformers, annotation, clustering and output formatting can now be performed with a single JAVA executable. This allows robust, coarsegrained linking of the FEPOPS computational core to various front and back end interfaces.

2.3. CombiAlign—FEPOPS combinatorial alignment

The original FEPOPS-I alignment mechanism relied upon charge distribution, rather than shape or geometry during the similarity calculations. The most negatively charged centroid was defined as feature point 1, whereas the most positively charged centroid was defined as feature point 4 (assuming initial selection of four k -means clusters) Here we introduce the concept of combinatorial alignment. To align two objects of four feature points it is sufficient to fix one of them and explore the combinations without repetition of the other one. Since the order of the feature points matters and each feature point can be chosen only once, then the number of permutations is given by Eq. (1), where n is the number of feature points from which we can choose and r is the number to be chosen.

$$\frac{n!}{(n-r)!} \quad (1)$$

Since $n = r = 4$ (meaning number of chosen feature points is equal to number of feature points to choose from) then the

formula becomes

$$\frac{n!}{(n-r)!} = \frac{n!}{0!} = n! = 4! = 24 \quad (2)$$

One of the advantages of the FEPOPS algorithm is its simplicity. Since it uses only a small number of feature points (typically four) to describe a compound there is no need to further reduce the size of the problem and all the putative alignments can be compared in an exhaustive manner. The alignment with the highest Pearson’s correlation value is presumed to be the proper one.

A powerful analytical advantage of this method was that the individual descriptors associated with each feature points could be included or excluded from the similarity calculation allowing for testing of single, or combined descriptor effects. For example, performing the above alignment using only the distance descriptors provides a rough “shape only” fitting of the molecules.

2.4. Database

The World of Molecular Bioactivity Database (WOMBAT) [23] (WOMBAT 2005 Sunset Molecular Systems; <http://sunsetmolecular.com/products/?id=4> (accessed on October 2006)) was used in this work. WOMBAT 2005.1 contains 117,007 compounds with 104,230 unique SMILES, which target 1021 unique proteins published in 4773 articles in medicinal chemistry journals between 1975 and 2004. Initially, only compounds with activity ($IC_{50}/EC_{50}/K_i/K_b/K_d/MIC/ED_{50}$) $< 30 \mu\text{m}$ were selected because this cutoff ensures reasonable potency while not resulting in a substantial loss of target information. Secondly, these were filtered to just those compounds having $IC_{50} < 30 \mu\text{m}$. Thus, two sets having 109,457/47,505 compounds with 964/544 biological targets were employed during this study. 3D descriptors were computed using the FEPOPS-I method as described previously [15].

2.5. Virtual screening for activity using nevirapine probe

Early studies employing scaled molecular representations for virtual screening, systematically compared feature points to a receptor derived grid to perform docking [7,8]. To relate FEPOPS ligand-based method of virtual screening to these previous works, the same molecular probe (HIV-1 reverse transcriptase (HIV-1 RT) inhibitor—nevirapine) was used.

2.5.1. 3D enrichment

The FEPOPS-I application generated 3D descriptors for the 47,505 compound, WOMBAT, test database as described above. A Pipeline Pilot protocol was built to perform Pearson’s correlation for assignment of similarity. A custom pilot script component was written to execute “CombiAlign” as described in Section 2.3. The FEPOPS representations of nevirapine were extracted and the pairwise Pearson’s correlations were calculated with respect to the remaining members of the

database. These calculations were performed in three ways: (1) the original method based upon charge alignment, (2) CombiAlign using all chemical descriptors and (3) CombiAlign using only distance descriptors (pseudo shape). For each method, compounds were sorted by maximal correlation and enrichments for ability to predict HIV-1 RT activity were plotted for presentation in Section 3.

2.5.2. 2D enrichment

The identical data set used for Section 2.5.1 was also processed for 2D similarity. SMILES from WOMBAT were read into Pipeline Pilot and both MDL public keys [24] and Extended Connectivity Fingerprint (ECFP_6) [18] descriptors were generated for all 47,505 compounds as described previously [15]. Using nevirapine as the reference molecule, Tanimoto similarity distance was computed for the remainder of the data. For each method, compounds were sorted by decreasing similarity and enrichment was calculated as in Section 2.5.1.

2.6. Analysis of ligand binding to cAMP-dependent protein kinase (PKA)

2.6.1. Preparation of conformer/tautomers

SMILES representation of tested compounds were read into Pipeline Pilot 5.0. Molecules were standardized for charge, and ionized at pH 7.4. Up to five tautomers were generated and enumerated for each molecule. Results were output to an SD formatted file for conformer generation.

The SD file was read into MOE 2006 [25] using the “Import Conformers” function with no input filters. Up to 250 conformers were generated for each tautomer using the following settings—Stochastic Search Strain Limit, 7; Superpose RMSD Test, 0.75; Refinement Conformation Limit, 300; Stochastic Search Failure Limit, 30; Stochastic Search Iteration Limit, 500; Energy Minimization Iteration Limit, 200; Energy Minimization Gradient Test, 0.1. No external constraints were applied to the force field potential. The MMFF 94 \times force field was employed with bonded and van der Waals terms enabled. MMFF charges were assigned, but electrostatic energies were specifically not included for energy calculations during conformer generation to broaden the resulting conformational pool [26]. Explicit hydrogens were retained using a custom script. Coordinates and annotation information were output to mol2 files as input for FEPOPS-II.

2.6.2. *k*-Means, *k*-medoids clustering and descriptor assignment

The mol2 file with MOE conformers was provided as input to the JAVA executable of FEPOPS-II. The executable partitioned ligand atoms into four *k*-mean clusters based upon their spatial coordinates. Centroids were defined from the atoms of each cluster. Partial charges of the atoms belonging to each cluster were summed and along with log *P*, hydrogen bond donors and acceptors were encoded into the centroids to create “feature points”. The distances between feature points were

recorded after sorting on the basis of quadrupole directionality to complete the FEPOPS descriptor.

Feature points clustering through *k*-medoids was performed to find a smaller number of representative conformers. Up to seven conformations for each of five tautomers were retained making a maximum of 35 different 3D structures possible for each unique 2D chemical entry. The full FEPOPS descriptor was used for medoid selection.

FEPOPS-II generation of descriptors and clustering of conformers for an average flexible molecule takes less than 0.6 s running under Linux on a 3.40 GHz Xeon server with 2GB physical memory. A test set of 253 drug-like molecules having 15,271 conformations was processed into FEPOPS conformers in 143 s including writing to disk.

2.6.3. Pearson's correlation and assignment of similarity

FEPOPS representations of ATP and balanol analogs were input to compute similarity indices for various alignments. As in Section 2.5, similarity was computed in three ways using: (1) the original method based upon charge alignment, (2) CombiAlign using all chemical descriptors and (3) CombiAlign using only distance descriptors (pseudo shape). In addition to similarity mapping based upon flexible models of the ATP probe, fitting was performed using the X-ray derived conformation of the bound ligand as rigid input.

2.6.4. Mapping of PKA site interactions

The 3D coordinates of PKA complexed with ligands ATP (1ATP) and balanol (1BAL) were downloaded from the RCSB PDB. To overlay binding sites, backbone atoms of residues Val15–Trp196 (728 atoms) were aligned using the “Match” function in Sybyl 7.1 with an RMSD of 0.92 Å. The Ligand Interaction Diagram (LID) feature in MOE 2006 was employed to look “under the hood” of the protein binding sites and produce a 2D scheme optimally representing the 3D ligand's interactions.

3. Results and discussion

Earlier studies employed scaled molecular representations to perform docking by systematically comparing feature points to a receptor derived grid [7,8]. Recognizing those successes fitting the HIV-1 reverse transcriptase (HIV-1 RT) inhibitor, nevirapine, to its receptor we chose to use this probe for an early test of FEPOPS for ligand-based virtual screening.

In ligand-based virtual screening, a researcher uses a molecule with known activity against a target of interest to locate “similar” molecules within a large data set (such as a company's compound collection). Typically, the entire database would be sorted by descending similarity and an “enrichment” factor determined from the percentage of all actives shifted to the top of the dataset relative to random distribution. Prospectively, such procedures may be used to cherry pick small subsets of molecules for experimental assay rather than screening an entire compound library.

Fig. 1 illustrates the comparative results of the three 3D method variations employed (1) the shape descriptor alone for

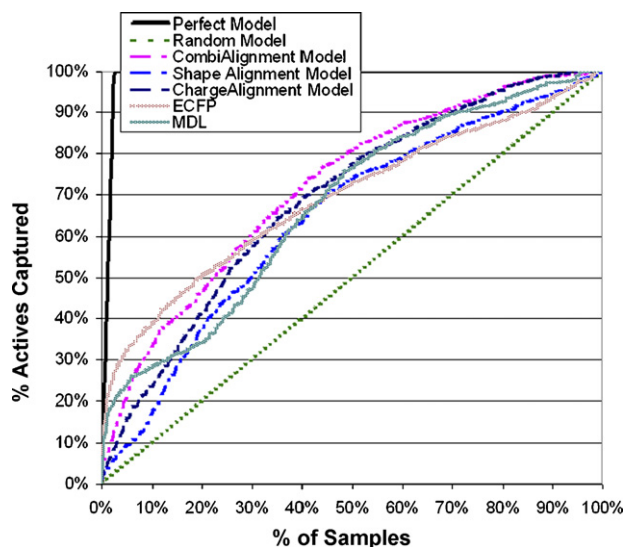
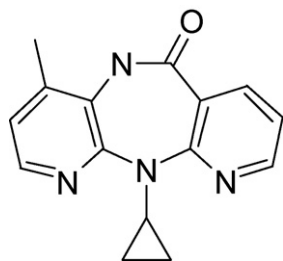


Fig. 1. Active recall using nevirapine probe and different alignment methods. Relative performance of three versions of FEPOPS and two 2D methods for selecting known HIV-RT actives from a background of over 47,000 other drug-like molecules using a single probe is shown. At the level of 10% sampled, shape matching to nevirapine (Scheme 2) was slightly better than random for separating actives and inactives. Charge based alignment performed better than shape for this molecular system. However, the combinatorial alignment method using both, charge and shape, as well as other descriptors out-performed both of the single descriptor 3D methods. The combinatorial 3D method also out performed the MDL keys and almost equaled ECFP enrichment for this system. Importantly, the compounds predicted by the 2D and 3D methods are not identical. It is also worth noting that this difficult dataset included a high percentage of structurally diverse actives which bind at the nucleotide site in addition to nevirapine's allosteric site. Non-competitive binders were not distinguished here, lowering apparent performance for all methods.

alignment and scoring, (2) charge based alignment and full descriptor scoring and (3) CombiAlign using all descriptors for alignment and scoring. Nevirapine (Scheme 2) was used as a single probe to rank molecules for HIV-1 RT activity within the 47,505 compound data set as described in Section 2. Performance, in this experiment, is judged as the relative ability to predict active compounds in the top 10% of the ranked dataset. It can be seen that the shape method registered the worst performance of the three for this system. The combinatorial method, using all six descriptors, resulted in about 30% increased enrichment relative to the charge based alignment. A closer comparison of the charge and combinatorial results are shown in Fig. 2. Importantly, more compounds with diverse chemical scaffolds were located in the first 300



Scheme 2. HIV-1 reverse transcriptase inhibitor—nevirapine.

molecules ranked for similarity and a representative set is shown. Discovering hits which break from the tricyclic core of the original molecule would be important to chemical teams developing new drugs. The poor performance using only shape for a small, relatively rigid molecule like nevirapine should not be a surprise. One can imagine that many small molecules could fit such a shape signature and that the placement of polar functional groups on that shape would be needed for biological recognition.

Consistent with previous findings for target fishing [15], both of the 2D methods shown in Fig. 1 produced better initial enrichments than the charge based version of FEPOPS. However, the combinatorial 3D method retrieves more actives than the MDL keys and shows performance near ECFP, while predicting different compounds than the 2D method. We view the 2D and 3D methods as complementary rather than competitive.

Given the rigidity of nevirapine as a chemical probe, we also explored the new alignment methods using more flexible probes such as ATP. A previous study in our lab, using FEPOPS-I for target identification, predicted a close 3D FEPOPS relationship between the structurally different PKA binders ATP and balanol (Scheme 3) [15]. In this study, we sought to compare the FEPOPS-II 3D conformer outputs relative to crystallographic complexes and to analyze differences in structural overlaps due to the choice of alignment. For this exercise, conformations of ATP and balanol analogs were generated within MOE 2006 and FEPOPS clustering was used to compress the chemical space of ATP as described in Section 2. Fig. 3 illustrates how the seven FEPOPS conformers compare to the 50 input conformers generated by MOE. Both charge based and combinatorial methods yielded high scoring (Pearson's value >0.94) alignments between the molecular pairs for all active analogs tested. The use of combinatorial alignment resulted in a higher score (Pearson's value = 0.97) and found a closely overlapping conformation with <0.9 Å RMSD between the aligned feature points as depicted in Fig. 4a. Importantly, this alignment (illustrated with color coding in Scheme 3 and Fig. 4c and d) was consistent with the orientation of the two ligands in the PKA binding site as determined experimentally [27,28]. However, ligands extracted from the superimposed protein structures do not show the same level of overlap as our ligand based search. What is the source of the discrepancy? Fig. 4c and d shows 2D representations of PKA site interactions from crystallographic complexes of the two drugs. The coloring scheme highlights ligand atom sets that were defined by FEPOPS *k*-means clustering. Same colored atom groups are predicted to be bioisosteric replacements. Accordingly, the A and B rings of balanol fill the subsites associated with ATP's adenine and ribose, respectively. The oxygen-rich rings C and D of balanol bridge similar interaction as ATP's triphosphate tail. 3D analysis of the same two sites reveals significant induced fit between these two ligands. The amide nitrogen of residue Ser 53 on the glycine rich loop moves nearly 3 Å to maintain contact between atoms of feature point 1 (red) in the different complexes. In fact, the centroids of feature point 1 for the two ligands in the aligned binding sites are over

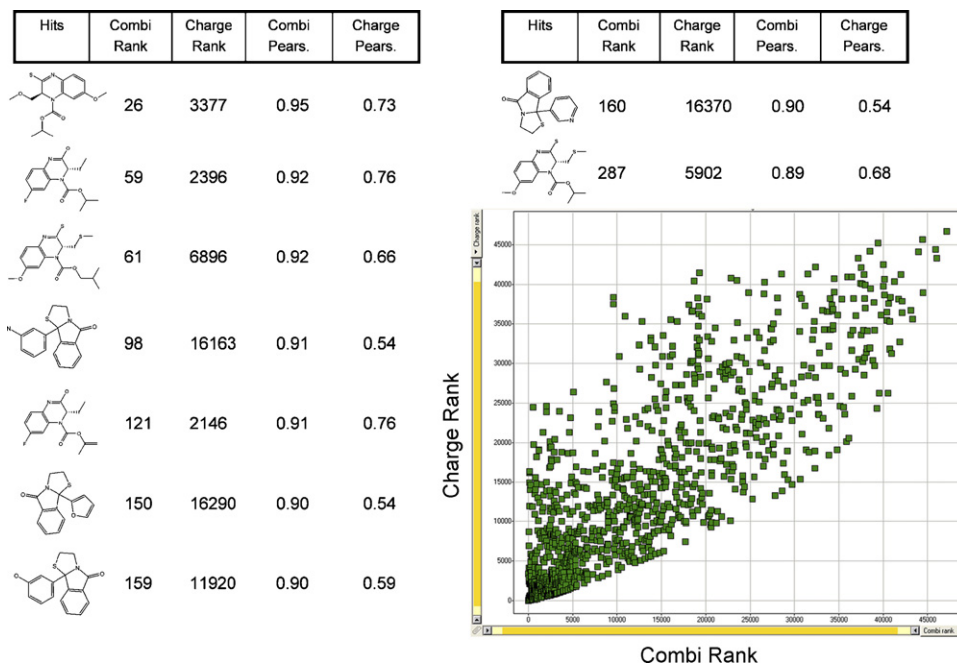
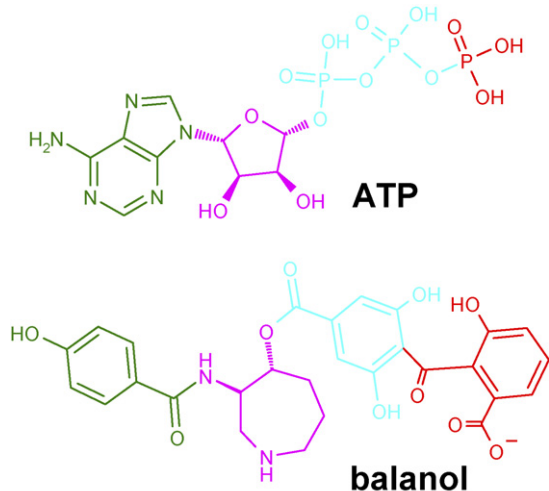


Fig. 2. Analysis of combinatorial vs. charge alignment for recall of HIV-RT actives. For each method, Pearson's correlations were used as similarity scores to rank each database compound relative to the nevirapine (Scheme 2) probe. The shape of the plot illustrates a significant improvement of early active recall for combinatorial alignment (Combi Rank). Importantly, the chemical representations show that a structural variety of "hits" were retrieved in the first 300 predicted molecules using the combinatorial method. Multiple representatives of new chemical classes were selected, so biological follow-up could inherently contain structure activity relationships that would be fed back into evolving pharmacophore models.

5 Å apart. Although, our flexible alignment reveals that ATP and balanol do have conformations which present similar features in space, their rigid biological space does not seem to match. For example, the bound conformation of ATP is significantly affected by the presence of manganese ions, not included in our search. Thus, in our flexible alignments, the best overlay of the two molecules most closely matches the bound conformation of balanol. (Carbons of the FEPOPS conformer of balanol overlay on the bound conformer with an RMSD < 1.5 Å.) Would FEPOPS find a match if we constrained the ATP probe to its conformation found in the

X-ray structure? The answer is yes. The top scoring tautomer/conformer aligns with a Pearson's value of 0.976—higher than when using the flexible conformers. We see this as the basis for the success this method has achieved in internal project work. *The pharmacophores are sufficiently flexible to match multiple states of dynamic biological sites.* Of particular interest for this example is that the best alignment coming from the combinatorial method with all descriptors is identical to that obtained using only distances that model shape. Charge, though certainly important for PKA biological activity, was not necessary for correct alignment in this limited case. However,



Scheme 3. ATP and balanol, a competitive inhibitor for select kinases. Color coding illustrates *k*-mean atomic clusters defining individual "feature points".

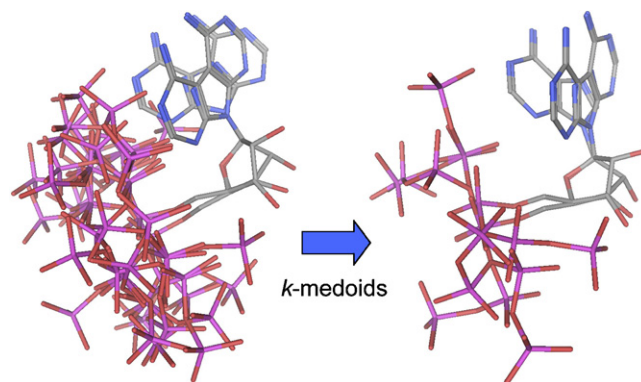


Fig. 3. Scaling down the conformational space of ATP by *k*-medoids clustering of the feature points. The full conformational set generated for a given molecule is reduced to a user defined number of "FEPOP conformers" through cluster based selection of distributed feature points. The default number of medoids employed in this study was *k* = 7.

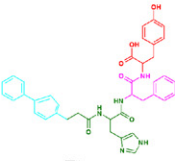
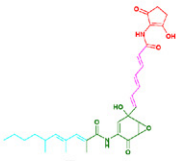
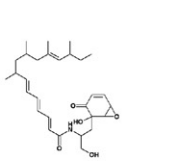
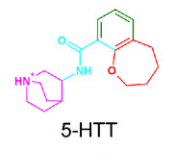
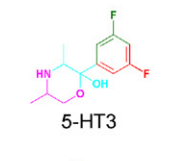
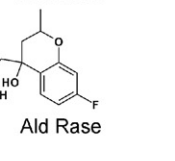
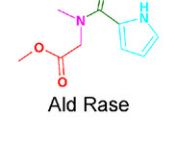
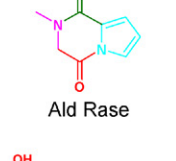
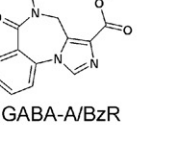
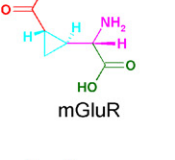
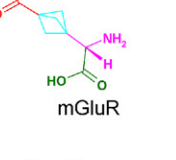
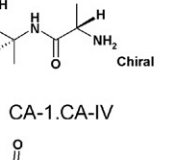
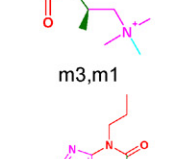
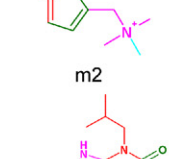
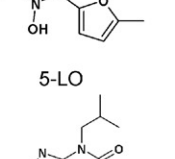
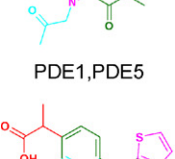
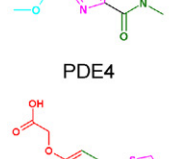
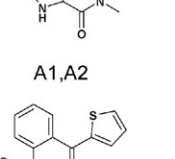
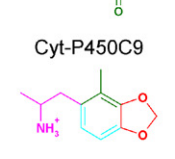

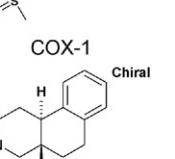
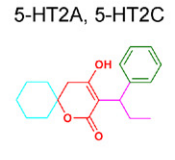
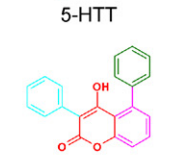
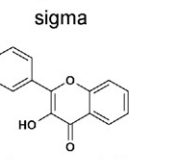
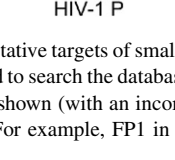
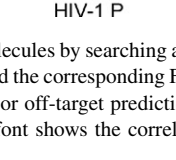
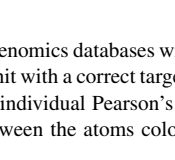
FEPOPS - hit	Probe	2D - hit	Pearson	FP-Similarity
			0.9614	Feature_Points FP1 = 0.999 FP2 = 0.991 FP3 = 1.000 FP4 = 0.442 Shape = 0.968
			0.8830	Feature_Points FP1 = 0.851 FP2 = -0.108 FP3 = 0.977 FP4 = 0.805 Shape = 0.889
			0.9451	Feature_Points FP1 = 0.964 FP2 = 1.000 FP3 = 0.935 FP4 = 1.000 Shape = 0.374
			0.9979	Feature_Points FP1 = 1.000 FP2 = 1.000 FP3 = 0.936 FP4 = 1.000 Shape = 0.990
			0.9906	Feature_Points FP1 = 0.953 FP2 = 0.993 FP3 = 1.000 FP4 = 0.999 Shape = 0.984
			0.8038	Feature_Points FP1 = 0.673 FP2 = 0.927 FP3 = 0.990 FP4 = 0.704 Shape = 0.811
			0.9825	Feature_Points FP1 = 0.999 FP2 = 0.912 FP3 = 0.589 FP4 = 1.000 Shape = 0.997
			0.9773	Feature_Points FP1 = 0.979 FP2 = 0.262 FP3 = 0.994 FP4 = 0.998 Shape = 0.898
			0.9671	Feature_Points FP1 = 0.989 FP2 = 0.907 FP3 = 0.982 FP4 = 0.998 Shape = 0.959

Fig. 5. Predicting the putative targets of small molecules by searching a chemogenomics databases with FEPOPS in cases where 2D similarity searching fails. (Left) The probe molecule used to search the database and the corresponding FEPOPS hit with a correct target (or close target homologue) prediction. The closest 2D match in the same database is shown (with an incorrect or off-target prediction). The individual Pearson's correlation values for feature points 1–4, as well as the shape correlation are shown. For example, FP1 in red font shows the correlation between the atoms color coded red in the probe and hit molecule.

present study, we have further computed the Pearson's correlations of the individual feature points of the probe and hit molecules. Additionally, the Pearson's correlation of distance descriptors are computed to obtain a "shape similarity" value. For example, in Fig. 5, row 2, FEPOPS

found a 5-HTT inhibitor in WOMBAT using a 5-HT3 inhibitor as a probe. Although the overall Pearson is 0.883, the individual contribution of feature point 2 (green) is negative. Feature point 2 atoms correspond to a portion of a phenyl ring in the hit molecule and a portion of a fluorophenyl ring in the probe

molecule. The sum of the Gasteiger charges of the atoms contributing to feature point 2 is quite different due to the presence of the fluorine atom. However, the remaining feature points and overall shape are similar enough to provide good overall FEPOPS similarity. The low score for feature point 2 carries us to a point in chemical space where there is some adaptability in the biological space. This also brings up the idea that partial alignment where some fractional number of feature points (example three out of four) could be used to exclude undesirable matches. As a second example, row #3 contains an aldose reductase inhibitor match. Although the overall shape is quite different (Shape Pearson = 0.374), feature points 1–4 are highly similar. In other words, poor matches in shape or individual feature point correlations can be compensated for, if the remaining descriptors are highly similar.

Numerous other methods exist for calculation of 3D similarity/superposition and/or pharmacophore elucidation and are reviewed elsewhere [30,31]. FEPOPS incorporates similar concepts in a way that lends itself to processing of large datasets—analogueous to high throughput screening (HTS). Any true 3D method has to address the issue of conformational flexibility. For FEPOPS, conformations may be either generated internally using fast torsional rotations with bump checking, or conformations may be derived from some external method. The unique feature of FEPOPS is that two layers of clustering are applied to reduce dimensionality of the 3D chemical data. Rather than using atomic alignments of two or more compound's to develop a pharmacophoric feature hypothesis, as in Catalyst or DISCO [32–34], FEature Point PharmacophoreS are simply chemical features mapped to *k*-means centroids from the atoms that define them. This reduces every conformation of every molecule to the same number of spatially separated pharmacophore points. The next level of *k*-medioid clustering reduces the broad conformational space to *k* conformers representing, spatially diverse chemical feature space. Therefore, each molecule's potential pharmacophores are predefined and written to a lookup table as shown in Scheme 1. No user curation of the pharmacophores is performed, nor is training based upon activity data. This simplification step is very fast. As reported in methods, reducing pre-computed conformers to FEPOPS descriptors and storing them takes less than 0.6 s per molecule. Generating internal conformations and clustering on that same data still adds less than 1 s per molecule. Having the same number of descriptors for each molecule allows rapid computation of a Pearson's correlation score. A new probe molecule may be tested against the precomputed descriptors of a 1 million compound library in less than 2 h using the combinatorial alignment algorithm described here. Although the current method has no automated way to evaluate the aligned pharmacophoric feature with respect to activity data as do Catalyst, DISCO, or the newer Phase [35], it is under development.

In this study, the compounds were prioritized by a decreasing Pearson's correlation value where all the descriptors had the same weight. We believe it will be of value to assign different statistical weights to each of the features depending upon the nature of the dataset and the biological target at hand.

Work is currently underway to train statistical models on aligned 3D features of bioactive molecular sets to extract weights for pharmacophore elucidation. A powerful aspect of feature points is that the user can increase the number to enhance the “shape” information. Using weights and/or partial shapes by only requiring subsets of features to align may be particularly useful for selecting between the binding and activating portions of antagonist and agonist or for modeling dynamic sites that bind molecule with non-traditional pharmacophores [36].

4. Conclusions

Graham Richards' early work significantly inspired modern research into chemical and biological similarity. Of particular importance to our lab is the use of clustering techniques and statistical analysis based on chemical descriptors to scale down the noise in large HTS datasets and to pull out the true signal [37]. Much excellent research has been done using 2D chemical similarity [11,12,38,39] and more 3D methods are emerging [13,40–45]. In this work, we show how clustering algorithms may be directly applied to 3D chemical structure and used to relate biological function. Our FEPOPS method reduces a small molecule's large, diverse, flexible, chemical space to a small number of feature clusters that may be rapidly compared with those of other molecules to predict functional similarity. We have shown that both shape and charge features can have significant influence on this predictivity, but *a priori* determination of important features is not obvious. To systematically explore these relations we have presented a new combinatorial alignment algorithm that considers multiple molecular feature descriptors during alignment and scoring. We have also developed a new 3D analysis environment where these overlapped chemical structures may be evaluated for patterns related to their biological activity. Further evaluation of these flexible pharmacophores over large well annotated data sets may afford addition insight into chemical function within dynamic biological environments.

Acknowledgements

We thank Alain Deschenes of Chemical Computing Group for additional scripting assistance. J.N. and A.B. thank the Education Office of NIBR for postdoctorate fellowship support.

References

- [1] J.C. Venter, M.D. Adams, E.W. Myers, P.W. Li, R.J. Mural, G.G. Sutton, H.O. Smith, M. Yandell, C.A. Evans, R.A. Holt, J.D. Gocayne, P. Amanatides, R.M. Ballew, D.H. Huseon, J.R. Wortman, Q. Zhang, C.D. Kodira, X.H. Zheng, L. Chen, M. Skupski, G. Subramanian, P.D. Thomas, J. Zhang, G.L. Gabor Miklos, C. Nelson, S. Broder, A.G. Clark, J. Nadeau, V.A. McKusick, N. Zinder, A.J. Levine, R.J. Roberts, M. Simon, C. Slayman, M. Hunkapiller, R. Bolanos, A. Delcher, I. Dew, D. Fasulo, M. Flanagan, L. Florea, A. Halpern, S. Hannenhalli, S. Kravitz, S. Levy, C. Mobarry, K. Reinert, K. Remington, J. Abu-Threideh, E. Beasley, K. Biddick, V. Bonazzi, R. Brandon, M. Cargill, I. Chandramouliswaran, R. Charlab, K. Chaturvedi, Z. Deng, V. Di Francesco, P. Dunn, K. Eilbeck, C. Evangelista, A.E. Gabrielian, W. Gan, W. Ge, F. Gong, Z. Gu, P. Guan, T.J.

- Heiman, M.E. Higgins, R.R. Ji, Z. Ke, K.A. Ketchum, Z. Lai, Y. Lei, Z. Li, J. Li, Y. Liang, X. Lin, F. Lu, G.V. Merkulov, N. Milshina, H.M. Moore, A.K. Naik, V.A. Narayan, B. Neelam, D. Nusskern, D.B. Rusch, S. Salzberg, W. Shao, B. Shue, J. Sun, Z. Wang, A. Wang, X. Wang, J. Wang, M. Wei, R. Wides, C. Xiao, C. Yan, A. Yao, J. Ye, M. Zhan, W. Zhang, H. Zhang, Q. Zhao, L. Zheng, F. Zhong, W. Zhong, S. Zhu, S. Zhao, D. Gilbert, S. Baumhueter, G. Spier, C. Carter, A. Cravchik, T. Woodage, F. Ali, H. An, A. Awe, D. Baldwin, H. Baden, M. Barnstead, I. Barrow, K. Beeson, D. Busam, A. Carver, A. Center, M.L. Cheng, L. Curry, S. Danaher, L. Davenport, R. Desilets, S. Dietz, K. Dodson, L. Doup, S. Ferreira, N. Garg, A. Gluecksmann, B. Hart, J. Haynes, C. Haynes, C. Heiner, S. Hladun, D. Hostin, J. Houck, T. Howland, C. Ibegwam, J. Johnson, F. Kalush, L. Kline, S. Koduru, A. Love, F. Mann, D. May, S. McCawley, T. McIntosh, I. McMullen, M. Moy, L. Moy, B. Murphy, K. Nelson, C. Pfannkoch, E. Pratts, V. Puri, H. Qureshi, M. Reardon, R. Rodriguez, Y.H. Rogers, D. Romblad, B. Ruhfel, R. Scott, C. Sitter, M. Smallwood, E. Stewart, R. Strong, E. Suh, R. Thomas, N.N. Tint, S. Tse, C. Vech, G. Wang, J. Wetter, S. Williams, M. Williams, S. Windsor, E. Winn-Deen, K. Wolfe, J. Zaveri, K. Zaveri, J.F. Abril, R. Guigo, M.J. Campbell, K.V. Sjolander, B. Karlak, A. Kejariwal, H. Mi, B. Lazareva, T. Hatton, A. Narechania, K. Diemer, A. Muruganujan, N. Guo, S. Sato, V. Bafna, S. Istrail, R. Lippert, R. Schwartz, B. Walenz, S. Yoosheph, D. Allen, A. Basu, J. Baxendale, L. Blick, M. Caminha, J. Carnes-Stine, P. Caulk, Y.H. Chiang, M. Coyne, C. Dahlke, A. Mays, M. Dombroski, M. Donnelly, D. Ely, S. Esparham, C. Fosler, H. Gire, S. Glanowski, K. Glasser, A. Glodek, M. Gorokhov, K. Graham, B. Gropman, M. Harris, J. Heil, S. Henderson, J. Hoover, D. Jennings, C. Jordan, J. Jordan, J. Kasha, L. Kagan, C. Kraft, A. Levitsky, M. Lewis, X. Liu, J. Lopez, D. Ma, W. Majoros, J. McDaniel, S. Murphy, M. Newman, T. Nguyen, N. Nguyen, M. Nodell, S. Pan, J. Peck, M. Peterson, W. Rowe, R. Sanders, J. Scott, M. Simpson, T. Smith, A. Sprague, T. Stockwell, R. Turner, E. Venter, M. Wang, M. Wen, D. Wu, M. Wu, A. Xia, A. Zandieh, X. Zhu, The sequence of the human genome, *Science* 291 (5507) (2001) 1304–1351.
- [2] J.L. DeRisi, V.R. Iyer, P.O. Brown, Exploring the metabolic and genetic control of gene expression on a genomic scale 10.1126/science.278.5338.680, *Science* 278 (5338) (1997) 680–686.
- [3] K. Palczewski, T. Kumasaka, T. Hori, C.A. Behnke, H. Motoshima, B.A. Fox, I. Le Trong, D.C. Teller, T. Okada, R.E. Stenkamp, M. Yamamoto, M. Miyano, Crystal structure of rhodopsin: A G protein-coupled receptor, *Science* 289 (5480) (2000) 739–745.
- [4] E. Nogales, S.G. Wolf, K.H. Downing, Structure of the alpha beta tubulin dimer by electron crystallography, *Nature* 391 (6663) (1998) 199–203.
- [5] S. Westermann, H.W. Wang, A. Avila-Sakar, D.G. Drubin, E. Nogales, G. Barnes, The Dam1 kinetochore ring complex moves processively on depolymerizing microtubule ends, *Nature* 440 (7083) (2006) 565–569.
- [6] J.A. DiMasi, R.W. Hansen, H.G. Grabowski, The price of innovation: new estimates of drug development costs, *J. Health Econ.* 22 (2) (2003) 151–185.
- [7] M. Glick, D.D. Robinson, G.H. Grant, W.G. Richards, Identification of ligand binding sites on proteins using a multi-scale approach, *J. Am. Chem. Soc.* 124 (10) (2002) 2337–2344.
- [8] M. Glick, G.H. Grant, W.G. Richards, Docking of flexible molecules using multiscale ligand representations, *J. Med. Chem.* 45 (21) (2002) 4639–4646.
- [9] G.L. Warren, C.W. Andrews, A.M. Capelli, B. Clarke, J. LaLonde, M.H. Lambert, M. Lindvall, N. Nevins, S.F. Semus, S. Senger, G. Tedesco, I.D. Wall, J.M. Woolven, C.E. Peishoff, M.S. Head, A critical assessment of docking programs and scoring functions, *J. Med. Chem.* 49 (20) (2006) 5912–5931.
- [10] Z. Deng, C. Chuaqui, J. Singh, Structural interaction fingerprint (SIFt): a novel method for analyzing three-dimensional protein–ligand binding interactions, *J. Med. Chem.* 47 (2) (2004) 337–344.
- [11] A. Bender, R.C. Glen, Molecular similarity: a key technique in molecular informatics, *Org. Biomol. Chem.* 2 (22) (2004) 3204–3218.
- [12] Y.C. Martin, J.L. Kofron, L.M. Traphagen, Do structurally similar molecules have similar biological activity? *J. Med. Chem.* 45 (19) (2002) 4350–4358.
- [13] J.L. Jenkins, M. Glick, J.W. Davies, A 3D similarity method for scaffold hopping from known drugs or natural ligands to new chemotypes, *J. Med. Chem.* 47 (25) (2004) 6144–6159.
- [14] K. Pearson, Mathematical contributions to the theory of evolution. III. Regression, heredity, and panmixia, *Philos. Trans. R. Soc. Lond. A Math. Phys. Eng. Sci.* 187 (1896) 253–318.
- [15] J.H. Nettles, J.L. Jenkins, A. Bender, Z. Deng, J.W. Davies, M. Glick, Bridging chemical and biological space: “target fishing” using 2D and 3D molecular descriptors, *J. Med. Chem.* 49 (2006) 6802–6810.
- [16] A.Y. Meyer, W.G. Richards, Similarity of molecular shape, *J. Comput. Aided Mol. Des.* 5 (5) (1991) 427–439.
- [17] T.S. Rush 3rd, J.A. Grant, L. Mosyak, A. Nicholls, A shape-based 3D scaffold hopping method and its application to a bacterial protein–protein interaction, *J. Med. Chem.* 48 (5) (2005) 1489–1495.
- [18] Pipeline Pilot, SciTegic, San Diego, CA, 2005.
- [19] J. Gasteiger, M. Marsili, Iterative partial equalization of orbital electronegativity—a rapid access to atomic charges, *Tetrahedron* 36 (22) (1980) 3219–3228.
- [20] R. Wang, Y. Fu, L. Lai, A new atom-additive method for calculating partition coefficients, *J. Chem. Inf. Model.* 37 (3) (1997) 615–621.
- [21] T. Hastie, R. Tibshirani, J. Friedman, *The Elements of Statistical Learning*, Springer, New York, 2001.
- [22] R.D.C. Team, R: A Language and Environment for Statistical Computing, R Foundation for Statistical Computing, Vienna, Austria, 2003.
- [23] M. Olah, M. Mracec, L. Ostropovici, R. Rad, A. Bora, N. Hadaruga, I. Olah, M. Banda, Z. Simon, M. Mracec, T.I. Oprea, WOMBAT: World of Molecular Bioactivity, in: T. Oprea (Ed.), *Chemoinformatics in Drug Discovery*, Wiley-VHC, New York, 2004, pp. 223–239.
- [24] MDL Public Keys, Elsevier MDL Inc., San Ramon, CA, 2001.
- [25] Molecular Operating Environment (MOE), Computational Computing Group, Montreal, Canada, 2006.
- [26] A. Lakdawala, M. Wang, N. Nevins, D.C. Liotta, D. Rusinska-Roszak, M. Lozynski, J.P. Snyder, Calculated conformer energies for organic molecules with multiple polar functionalities are method dependent: Taxol (case study), *BMC Chem. Biol.* 1 (1) (2001) 2.
- [27] N. Narayana, T.C. Diller, K. Koide, M.E. Bunnage, K.C. Nicolaou, L.L. Brunton, N.H. Xuong, L.F. Ten Eyck, S.S. Taylor, Crystal structure of the potent natural product inhibitor balanol in complex with the catalytic subunit of cAMP-dependent protein kinase, *Biochemistry* 38 (8) (1999) 2367–2376.
- [28] J.H. Zheng, E.A. Trafny, D.R. Knighton, N.H. Xuong, S.S. Taylor, L.F. Teneyck, J.M. Sowadski, 2.0 Å refined crystal-structure of the catalytic subunit of cAMP-dependent protein-kinase complexed with Mg ATP and a peptide inhibitor, *Acta Crystallogr. D Biol. Crystallogr.* 49 (1993) 362–365.
- [29] Nidhi, M. Glick, J.W. Davies, J.L. Jenkins, Prediction of biological targets for compounds using multiple-category Bayesian models trained on chemogenomics databases, *J. Chem. Inf. Model.* 46 (3) (2006) 1124–1133.
- [30] O.F. Guner, *Pharmacophore Perception, Development and Use in Drug Design*, International University Line, La Jolla, 2000.
- [31] C. Lemmen, T. Lengauer, Computational methods for the structural alignment of molecules, *J. Comput. Aided Mol. Des.* 14 (3) (2000) 215–232.
- [32] O.O. Clement, A.T. Mehl, HipHop: pharmacophores based on multiple common-feature alignments, in: O.F. Guner (Ed.), *Pharmacophore Perception, Development and Use in Drug Design*, International University Line, La Jolla, 2000, pp. 69–84.
- [33] Y.C.D. Martin, What We Did Right and What We Missed, in: O.F. Guner (Ed.), *Pharmacophore Perception, Development and Use in Drug Design*, International University Line, La Jolla, 2000, pp. 51–68.
- [34] Y. Patel, V.J. Gillet, G. Bravi, A.R. Leach, A comparison of the pharmacophore identification programs: Catalyst, DISCO and GASP, *J. Comput. Aided Mol. Des.* 16 (8/9) (2002) 653–681.
- [35] S.L. Dixon, A.M. Smondyrev, E.H. Knoll, S.N. Rao, D.E. Shaw, R.A. Friesner, PHASE: a new engine for pharmacophore perception, 3D QSAR model development, and 3D database screening. 1. Methodology and

- preliminary results, *J. Comput. Aided Mol. Des.* 20 (10–11) (2006) 647–671.
- [36] J.H. Nettles, H. Li, B. Cornett, J.M. Krahn, J.P. Snyder, K.H. Downing, The binding mode of epothilone A on alpha, beta-tubulin by electron crystallography, *Science* 305 (5685) (2004) 866–869.
- [37] M. Glick, J.L. Jenkins, J.H. Nettles, H. Hitchings, J.W. Davies, Enrichment of high-throughput screening data with increasing levels of noise using support vector machines, recursive partitioning, and laplacian-modified naive bayesian classifiers, *J. Chem. Inf. Model.* 46 (1) (2006) 193–200.
- [38] J. Hert, P. Willett, D.J. Wilton, P. Acklin, K. Azzaoui, E. Jacoby, A. Schuffenhauer, Comparison of topological descriptors for similarity-based virtual screening using multiple bioactive reference structures, *Org. Biomol. Chem.* 2 (22) (2004) 3256–3266.
- [39] J. Hert, P. Willett, D.J. Wilton, P. Acklin, K. Azzaoui, E. Jacoby, A. Schuffenhauer, Comparison of fingerprint-based methods for virtual screening using multiple bioactive reference structures, *J. Chem. Inf. Comput. Sci.* 44 (3) (2004) 1177–1185.
- [40] C. Lemmen, T. Lengauer, G. Klebe, FLEXS: a method for fast flexible ligand superposition, *J. Med. Chem.* 41 (23) (1998) 4502–4520.
- [41] G. Schneider, W. Neidhart, T. Giller, G. Schmid, Scaffold-hopping by topological pharmacophore search: a contribution to virtual screening, *Angew. Chem. Int. Ed. Engl.* 38 (19) (1999) 2894–2896.
- [42] A.N. Jain, Morphological similarity: a 3D molecular similarity method correlated with protein–ligand recognition, *J. Comput. Aided Mol. Des.* 14 (2) (2000) 199–213.
- [43] R.D. Cramer, R.J. Jilek, K.M. Andrews, dbtop: Topomer similarity searching of conventional structure databases, *J. Mol. Graph. Modell.* 20 (6) (2002) 447–462.
- [44] A. Nicholls, N.E. MacCuish, J.D. MacCuish, Variable selection and model validation of 2D and 3D molecular descriptors, *J. Comput. Aided Mol. Des.* 18 (7–9) (2004) 451–474.
- [45] G. Wolber, T. Langer, LigandScout: 3D pharmacophores derived from protein-bound ligands and their use as virtual screening filters, *J. Chem. Inf. Model.* 45 (1) (2005) 160–169.